

# Seasonal ITCZ migration dynamically controls the location of the (sub)tropical Atlantic biogeochemical divide

Christian Schlosser<sup>a,1</sup>, Jessica K. Klar<sup>a</sup>, Bronwyn D. Wake<sup>a</sup>, Joseph T. Snow<sup>a</sup>, David J. Honey<sup>a</sup>, E. Malcolm S. Woodward<sup>b</sup>, Maeve C. Lohan<sup>c</sup>, Eric P. Achterberg<sup>a,d</sup>, and C. Mark Moore<sup>a,1</sup>

<sup>a</sup>Ocean and Earth Sciences, National Oceanography Centre Southampton, University of Southampton, Southampton SO14 3ZH, United Kingdom;

<sup>b</sup>Department of Nutrient Cycling, Plymouth Marine Laboratory, Plymouth PL1 3DH, United Kingdom; <sup>c</sup>School of Geography, Earth and Environmental Sciences, University of Plymouth, Plymouth PL4 8AA, United Kingdom; and <sup>d</sup>GEOMAR Helmholtz-Zentrum für Ozeanforschung, 24148 Kiel, Germany

Edited by Paul G. Falkowski, Rutgers, The State University of New Jersey, New Brunswick, NJ, and approved November 25, 2013 (received for review October 4, 2013)

Inorganic nitrogen depletion restricts productivity in much of the low-latitude oceans, generating a selective advantage for diazotrophic organisms capable of fixing atmospheric dinitrogen (N<sub>2</sub>). However, the abundance and activity of diazotrophs can in turn be controlled by the availability of other potentially limiting nutrients, including phosphorus (P) and iron (Fe). Here we present high-resolution data (~0.3°) for dissolved iron, aluminum, and inorganic phosphorus that confirm the existence of a sharp north-south biogeochemical boundary in the surface nutrient concentrations of the (sub)tropical Atlantic Ocean. Combining satellite-based precipitation data with results from a previous study, we here demonstrate that wet deposition in the region of the intertropical convergence zone acts as the major dissolved iron source to surface waters. Moreover, corresponding observations of N<sub>2</sub> fixation and the distribution of diazotrophic *Trichodesmium* spp. indicate that movement in the region of elevated dissolved iron as a result of the seasonal migration of the intertropical convergence zone drives a shift in the latitudinal distribution of diazotrophy and corresponding dissolved inorganic phosphorus depletion. These conclusions are consistent with the results of an idealized numerical model of the system. The boundary between the distinct biogeochemical systems of the (sub)tropical Atlantic thus appears to be defined by the diazotrophic response to spatial-temporal variability in external Fe inputs. Consequently, in addition to demonstrating a unique seasonal cycle forced by atmospheric nutrient inputs, we suggest that the underlying biogeochemical mechanisms would likely characterize the response of oligotrophic systems to altered environmental forcing over longer timescales.

nitrogen fixation | atmospheric iron deposition

Within the majority of the oligotrophic (sub)tropical regions of the surface ocean, bioavailable forms of fixed nitrogen (N) are severely depleted, restricting microbial biomass and productivity (1–3). Organisms capable of fixing atmospheric dinitrogen (N<sub>2</sub>) thus potentially have a considerable selective advantage in these vast N-limited environments (2), with the combined activity of these diazotrophs subsequently being responsible for maintaining the oceanic fixed-N inventory and, hence, overall productivity (1, 2, 4). Although clearly not susceptible to N limitation, in common with all living organisms, oceanic diazotrophs have an absolute requirement for a wide range of other nutrient elements, including phosphorus (P) and iron (Fe) (5). Indeed, diazotrophs have an enhanced requirement for the micronutrient Fe (6–8) due to the absolute requirement for this element within nitrogenase, the catalyst responsible for N<sub>2</sub> fixation (1, 9, 10). It has consequently been suggested that Fe availability may play a major role in controlling oceanic N<sub>2</sub> fixation (1, 11).

In contrast to the ubiquitous depletion of dissolved inorganic nitrogen (DIN), surface concentrations of dissolved Fe (DFe) and inorganic P (DIP) vary greatly among different regions of the

oligotrophic low-latitude oceans (12–14). Marked regional differences in N<sub>2</sub> fixation are also observed (15) and, in combination, such observations have been argued to support the hypothesis that diazotrophy can be enhanced in regions of high-Fe inputs, resulting in subsequent drawdown of DIP (12, 13, 16). Although an ever-growing body of evidence supports the importance of Fe for diazotrophy (9, 12, 14, 17), artificial in situ tests comparable to those that unequivocally demonstrated the Fe limited status of high-nitrate low-chlorophyll (HNLC) regions (18) have yet to be performed. Indeed, the slow response timescales of some diazotrophs may ultimately render such experiments unfeasible (19, 20).

The interactions among Fe, DIP, and diazotroph activity appear particularly evident in the low-latitude oligotrophic surface waters of the Atlantic Ocean (12, 17). Iron is highly insoluble and rapidly scavenged from oxic seawater (21). In consequence, the availability of this micronutrient in surface waters is often tightly coupled to external sources, including inputs of terrigenous materials via aeolian deposition (22–24). The (sub)tropical North Atlantic receives the highest deposition fluxes of aeolian dust in the global ocean (22) and is characterized by relatively high DFe (25, 26), with corresponding severe DIP depletion argued to result from significant diazotrophic activity either within or upstream of this system (12, 13). In contrast, the (sub)tropical South Atlantic gyre is characterized by relatively high DIP and very low DFe concentrations

## Significance

Low concentrations of fixed nitrogen restrict phytoplankton growth in much of the low-latitude surface oceans. Diazotrophic cyanobacteria are capable of fixing atmospheric dinitrogen, thereby replenishing the overall pool of fixed nitrogen. As a consequence, spatial-temporal variability in diazotrophy can potentially influence the global nitrogen cycle. Here we show that movement in the region of elevated iron concentrations tied to the seasonal migration of the intertropical convergence zone drives a shift in the latitudinal distribution of dinitrogen fixation and corresponding phosphate depletion in surface waters. Surface nutrient concentrations and diazotrophic activity divide the (sub)tropical Atlantic into a high-phosphate, low-iron system in the south, and a low-phosphate, high-iron system in the north.

Author contributions: C.S., E.P.A., and C.M.M. designed research; C.S., J.K.K., B.D.W., J.T.S., D.J.H., E.M.S.W., M.C.L., E.P.A., and C.M.M. performed research; C.S., J.K.K., E.P.A., and C.M.M. analyzed data; and C.S., E.M.S.W., M.C.L., E.P.A., and C.M.M. wrote the paper.

The authors declare no conflict of interest.

This article is a PNAS Direct Submission.

See Commentary on page 1231.

<sup>1</sup>To whom correspondence may be addressed. E-mail: C.Schlosser@noc.soton.ac.uk or cmm297@noc.soton.ac.uk.

This article contains supporting information online at [www.pnas.org/lookup/suppl/doi:10.1073/pnas.1318670111/-DCSupplemental](http://www.pnas.org/lookup/suppl/doi:10.1073/pnas.1318670111/-DCSupplemental).

(12, 27, 28). The boundary region between these (sub)tropical gyre systems is typically characterized by high rates of  $N_2$  fixation, which are dominated by the diazotrophic cyanobacterium *Trichodesmium* spp. (12, 29–31), and appear to be spatially correlated with some of the areas of highest DFe concentrations (12). Surface nutrient concentrations and diazotrophic activity thus appear to define a biogeochemical division of the Atlantic between a high DIP, low DFe (HPLFe) system in the south, and a low DIP, high DFe (LPHFe) system in the north (12).

Although the biogeochemical division of the (sub)tropical Atlantic has previously been interpreted on the basis of the hypothesized Fe control of diazotrophy (12, 13), there remains the possibility that the observed spatial patterns could have other forcing factors (32). Moreover, the wider regional and global importance of Fe controls on diazotrophy in both the modern and paleo ocean remains a matter of active debate (12, 17, 33–35) with important implications for our understanding of, for example, glacial/interglacial nitrogen and carbon cycling (1, 36–38). More direct tests of the Fe–diazotrophy limitation hypothesis are thus desirable. In particular, predictable large-scale dynamic responses of marine diazotrophy and subsequent P cycling to seasonal variability in external Fe inputs has not previously been described.

## Results and Discussion

The Sahara and Sahel deserts deliver large quantities of mineral dust to the (sub)tropical North Atlantic (22, 39). Tropical Rainfall Measuring Mission (TRMM) and Moderate Resolution Imaging Spectroradiometer (MODIS) satellite data for the period of our research cruise (February–March 2011), indicated that the northern part of the study region received significant dry (Fig. 1A) and wet (Fig. 1B) atmospheric deposition fluxes. However, the tropical South Atlantic was strongly shielded from desert dust by the InterTropical Convergence Zone (ITCZ), which had its core at  $\sim 1^\circ N$  during our cruise period, close to the southernmost latitude reached during its annual migration (40, 41) (Fig. 1B). In contrast, during a previous study in the region (October–November 2005; Atlantic Meridional Transect [AMT-17]; ref. 42) the ITCZ was located at  $\sim 6^\circ N$ , nearer to the northernmost extent (Fig. 1C).

The low pressure system of the ITCZ, formed by rapidly rising humid air (41), is characterized by heavy precipitation of up to  $\sim 0.8 \text{ mm h}^{-1}$  (43) (Fig. 1B and C). Aerosols are rapidly scavenged by this band of precipitation (24, 44), and the ITCZ system also restricts southward transport of desert-dust-rich air masses, as was evidenced by air mass back trajectories (HYbrid Single-Particle Lagrangian Integrated Trajectory [HYSPPLIT]) calculated for the periods of both cruises (Fig. S1). Precipitation has a major influence on sea surface salinity (SSS) in the tropical Atlantic, with the latitudinal migration of the ITCZ (40, 41) resulting in a strong seasonal cycle in local salt storage in the region between  $\sim 0^\circ$  and  $10^\circ N$  (45, 46). Correspondingly, we observed that the core of the ITCZ was associated with SSS minima during both meridional transects in 2005 and 2011 (Fig. 2).

Wet deposition within the ITCZ has previously been proposed to dominate trace metal inputs in the region (24, 47). Correspondingly, we observed that dissolved aluminum (DAI), a non-nutrient tracer of atmospheric inputs (24, 48) and the micronutrient DFe were highly correlated both with each other and with SSS along our two high-resolution 2011 transects (Fig. 2). The relationship of DFe and DAI with SSS for the earlier 2005 transect was remarkably similar (Fig. S2), despite a  $\sim 4^\circ$  latitudinal offset in the region of minimum SSS and maximum DFe and DAI concentrations.

Tighter correlation between DFe and precipitation (Fig. 1B) and SSS (Fig. 2), rather than aerosol optical thickness (Fig. 1A), suggest that wet deposition dominated Fe input in this region. More efficient solubilization of Fe from mineral dust particles during wet deposition (49, 50) due to a low rainwater pH

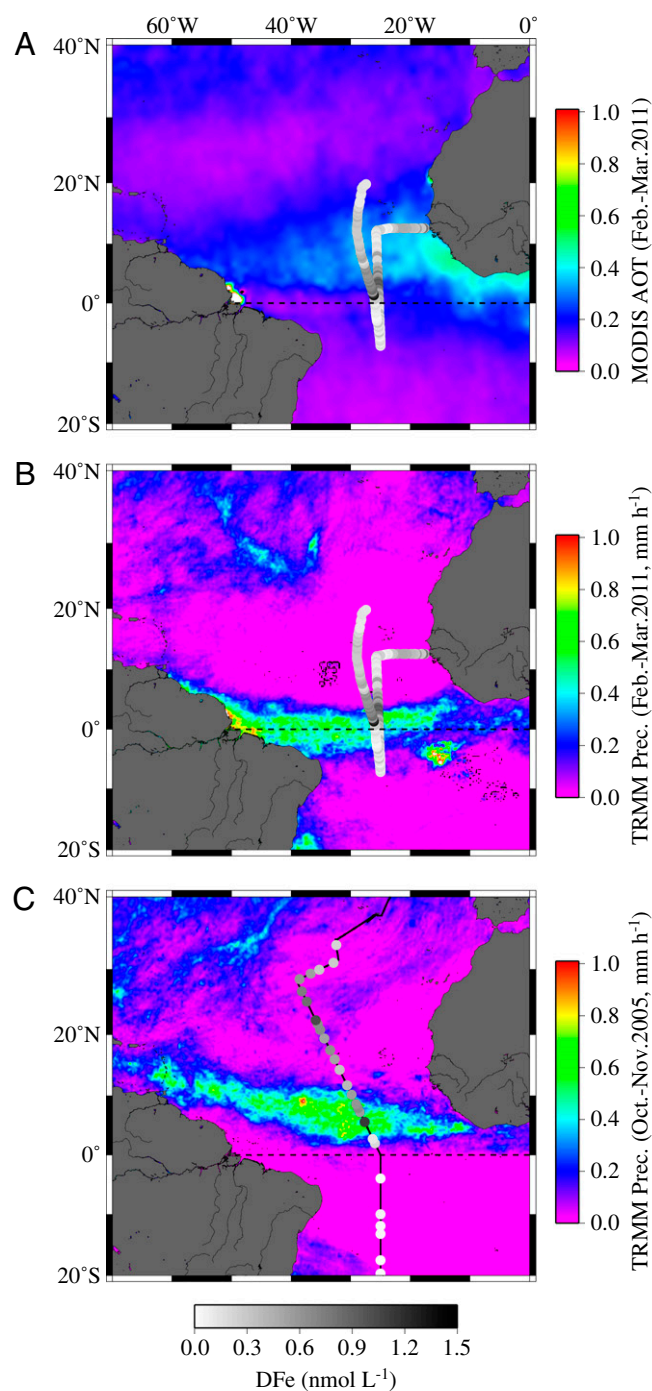


**Fig. 1.** (A) Aerosol optical thickness (AOT) recorded by the MODIS satellite at 550 nm during February and March 2011. B and C illustrate satellite rainfall rates (TRMM) determined during D361 between February and March 2011 and during AMT-17 between October and November 2005. The black lines indicate the general cruise track and the gray circles the dissolved Fe concentration for surface samples collected in February–March 2011 (A and B) and October–November 2005 (C). The dashed line indicates the equator.

(pH 4–6), the presence of Fe-binding ligands (51), and continuous photochemical reactions producing soluble Fe(II) in rain droplets (49) may all contribute to such dominance. Our data (Fig. 2), together with previous observations (12, 24, 47), thus strongly argue for wet deposition associated with the ITCZ forming the major source of DFe to the surface waters of the tropical Atlantic, as the ITCZ simultaneously shields the South

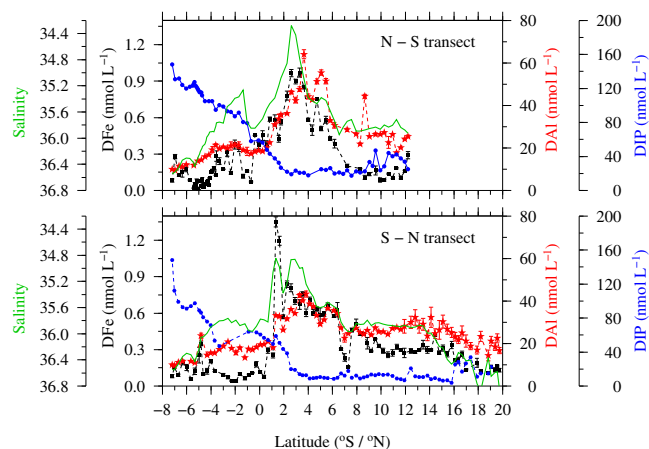


**Fig. 2.** Shown are the courses of DFe, DAI, and SSS in reverse scale, and DIP determined during D361 between 7°S and 20°N for the north-south (Upper) and south-north transect (Lower). Error bars represent the SD of triplicate measurements.

Atlantic from atmospheric dust inputs, resulting in low DFe concentrations (12, 28).

Sharp gradients in surface water DIP corresponded with the southern boundaries of the regions of minimum SSS and enhanced DFe in 2011 (Fig. 2). The inverse relationship between DFe and DIP thus agreed with our 2005 observations (12); however, the strong gradient region was offset to the south by 5°–10°, corresponding to the seasonal southward displacement of the ITCZ (Fig. 3). Moreover, observed  $N_2$ -fixation rates, alongside the abundance of *Trichodesmium*, peaked in the broad transition region between the HPLFe waters to the south and the LPHFe waters to the north in 2011 and 2005, thus demonstrating an apparent seasonal latitudinal shift consistent with previous data from the region (52). Consequently, data from three crossings of the ITCZ (Figs. 2 and 3) were fully consistent with our proposed conceptual model, whereby spatiotemporal variability in Fe inputs can drive variability in diazotrophy and subsequently control the availability of excess DIP in a system (12, 13).

To further illustrate the plausibility of the proposed mechanism, we expanded a widely used simple numerical model (53–55) to incorporate an idealized two-layer (surface-thermocline) horizontal transport framework, which can be taken to represent interactions between differential nutrient supplies (N, P, and Fe) and (non)diazotrophs along any generic upper-ocean circulation pathway (*SI Materials and Methods*). In the current case, our model configuration can be considered an idealized representation of the upper limb of the Atlantic overturning circulation (12, 56), where surface and thermocline waters apparently accumulate geochemical and isotopic imprints of  $N_2$  fixation during this large-scale northward transport (12, 57). Although simple, the underlying functional equations (55) are effectively identical to those used within more complex biogeochemical/ecosystem general circulation models (58, 59). In consequence, the qualitative behavior is expected to be consistent with more complex circulation and ecosystem scenarios, and the responses to variable forcing will be more fully tractable.

Qualitative steady-state outputs from our model setup were highly insensitive to parameter choices within well-defined bounds (Table S1). Thus, running the model with an initial subsurface excess of DIP, as occurs almost ubiquitously throughout the global (sub)tropical oceans (4, 55), and a spatially varying Fe input, specifically a peak (or equivalently a jump) in input, resulted in different areas of the model domain corresponding to two well-defined regimes. Specifically, a “switch” occurs between a modeled initial HPLFe and subsequent LPHFe condition (Fig. S3), with the

boundary region of this switch, a biogeochemical divide, being related to the external Fe input and associated with a corresponding peak in diazotrophy (Fig. S4). Formally, this occurs because diazotrophy increases sharply at the location in the model domain where the ratio of total Fe:DIN inputs is sufficient to maintain surface DFe concentrations above the corresponding equilibrium resource concentration for diazotrophs, typically denoted  $R^*_{Fe}$  (55).

As previously noted (55), steady-state model outputs were highly analogous to the observed situation in the Atlantic, with the added two-layer horizontal transport framework providing additional realism to the current configuration. Because the peak in diazotrophy is collocated with a critical increase in external Fe input, this would be expected to track Fe inputs at steady state. Further, within dynamic model runs incorporating a temporal variability in the region of enhanced Fe input (Fig. S4), i.e., analogous to the latitudinal movement of the ITCZ, the region of enhanced diazotrophy and hence the location of the biogeochemical divide between HPLFe and LPHFe waters, tracks the shifting Fe input in a manner that is qualitatively indistinguishable from the data of our seasonally separated transects (Fig. 3).

Although highly significant biogeochemical responses to seasonal variability in heat input, mixing, and light availability are well known in the open ocean (60, 61), we provide a fully supported description of a large-scale biogeochemical response to seasonal forcing by spatial-temporal variability in external, specifically atmospheric, nutrient inputs. Our results also have important implications beyond the demonstrated seasonal and regional scales. Despite the current lack of comprehensive surface ocean DFe data, the contrasting HPLFe and LPHFe conditions that characterize the South and North Atlantic subtropical gyres (12, 13, 28) appear to be representative of the large-scale biogeochemistry of the entire oligotrophic (low bioavailable fixed N) (sub)tropical oceans (14, 15, 55). Understanding the processes responsible for this large-scale biogeochemical partitioning is thus of global significance.

Conceptually predictable dynamic responses (Fig. 3) can provide stronger evidence of causation than can be provided by simple correlative studies (12). Consequently, our observations build on those of smaller-event-scale responses of diazotrophs to dust inputs (62, 63). It is crucial to note that the variability in Fe inputs due to the migration of the ITCZ appears to occur over sufficient spatial and temporal scales that the system is driven fully from the HPLFe to the LPHFe state, over a 300–400 km latitudinal band just north of the equator (Fig. 3). The current study thus potentially represents the closest possible analogy to the type of deliberate large-scale Fe releases that would demonstrate diazotroph-Fe limitation, in a similar manner to that achieved in the HNLC systems, but which may be practically and politically unfeasible over the long timescales required for fully developed diazotrophic responses (20).

The dynamic response to increased external Fe inputs we describe here thus strongly supports the importance of Fe availability for diazotrophy (1, 11), with consequent excess DIP removal to the point where this subsequently becomes the limiting resource (12, 13, 55). The broad basin-scale biogeochemical partitioning of the oligotrophic oceans into HPLFe and LPHFe regions is thus proposed to be a reciprocal consequence and driver of diazotrophic activity, with enhanced rates of diazotrophy both predicted and observed to occur at the boundaries of these regions (55) (Fig. 3). Continued interpretation of the local, regional, and potentially even the global balance between fixed N loss from the oceans through the processes of denitrification/anaerobic ammonium oxidation and inputs through  $N_2$  fixation (1, 4, 34, 36) will thus need to simultaneously consider spatial patterns of both excess P and Fe availability, as well as variability in these patterns, over multiple timescales. For example, climatic migration of the ITCZ (64) may interact with both regional (38) and remotely forced

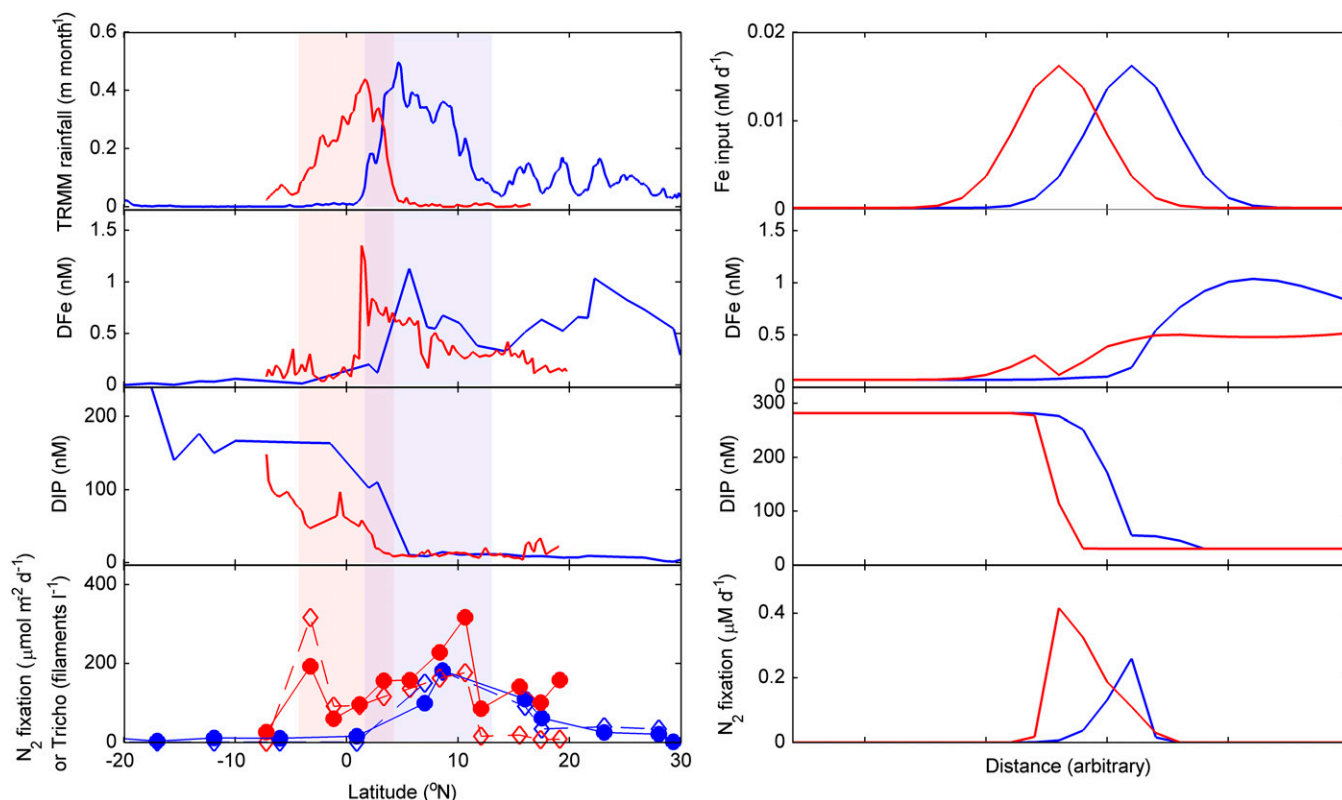


**Fig. 3.** (Left) Data from the AMT-17 (blue) and D361 (red) cruises for satellite derived rainfall, surface DFe, surface DIP, and depth-integrated  $N_2$  fixation (solid symbols) and *Trichodesmium* spp. abundance (open symbols). (Right) Output from example dynamic model run forced with spatially varying near surface iron inputs. Outputs correspond to two different time intervals corresponding to maximum spatial offsets in region of peak Fe input.

(36, 37) variability in excess P supply, to influence the activity of diazotrophs in the Atlantic (65). Removal of excess P within the Fe-rich North Atlantic is potentially also important in the maintenance of a global-scale coupling between the N and P cycles (12, 38). Indeed, Fe controls on large-scale diazotroph biogeography may be essential in allowing the negative feedbacks proposed to stabilize the N inventory over long timescales (53, 66) to operate, through partially decoupling regions of fixed N inputs and losses, hence preventing runaway N loss (67, 68).

Seasonal shifts in the ITCZ and associated wet deposition dominated Fe inputs appeared to dynamically control diazotrophy and reciprocal feedbacks to the nutrient biogeochemical divide of the tropical Atlantic, in a manner which was entirely predictable on the basis of simple theory as encapsulated in an idealized numerical model. Such detailed observations of dynamic responses to alterations in natural external forcing, coupled with conceptual mechanistic understanding of the processes involved, not only provides a powerful means for understanding the modern oceans, but will also allow better predictions of biogeochemical responses to multifaceted global change both in the past and future.

## Materials and Methods

**Water Sampling.** Trace-metal-clean surface seawater samples were collected during the UK GA06 GEOTRACES cruise (D361) on the UK research ship *RRS Discovery*. The cruise took place between February and March 2011 in

the (sub)tropical Atlantic Ocean and covered an area between 27°N–7°S and 17°–28°W.

**Treatment and On-Board Measurements.** All collected DIP samples were analyzed immediately on board with a nanomolar phosphate method using a segmented flow colorimetric analyzer with 2-m liquid waveguide flowcell (69). Dissolved Fe was determined using flow injection analysis (FIA) with luminol chemiluminescence (70). Dissolved Al concentrations were analyzed using FIA with the lumogallion-Al fluorescence technique (71).  $N_2$  fixation was measured using the  $^{15}N_2$  technique (72) following similar procedures to those described elsewhere (17, 73).

**Numeric Model.** The model simulates the interactions between two broad planktonic groups of phytoplankton and diazotrophs in competition for three nutrients (N, P, and Fe) (Fig. S5). The differential equations describing the evolution of the state variables were effectively identical to those used by Ward et al. (55). See the supporting information (*SI Materials and Methods*) for more detailed information about the model, sample handling, the DFe and DAI techniques,  $N_2$  fixation and associated uncertainties (Fig. S6), and *Trichodesmium* spp. abundances.

**ACKNOWLEDGMENTS.** We thank the captain and crew of *RRS Discovery*. Special thanks to Dr. Angela Milne and Felix Morales for help sampling seawater. Thanks to the two reviewers for their helpful comments. This project was funded by the UK National Environmental Research Council (NE/G015732/1) and the Atlantic Meridional Transect consortium (243).

- Falkowski PG (1997) Evolution of the nitrogen cycle and its influence on the biological sequestration of  $CO_2$  in the ocean. *Nature* 387(6630):272–275.
- Zehr JP, Kudela RM (2011) Nitrogen cycle of the open ocean: from genes to ecosystems. *Annu Rev Mar Sci* 3:197–225.
- Moore CM, et al. (2013) Processes and patterns of oceanic nutrient limitation. *Nat Geosci* 6(9):701–710.
- Deutsch C, Sarmiento JL, Sigman DM, Gruber N, Dunne JP (2007) Spatial coupling of nitrogen inputs and losses in the ocean. *Nature* 445(7124):163–167.

- Tovar-Sanchez A, et al. (2006) Effects of dust deposition and river discharges on trace metal composition of *Trichodesmium* spp. in the tropical and subtropical North Atlantic Ocean. *Limnol Oceanogr* 51(4):1755–1761.
- Berman-Frank I, Cullen JT, Shaked Y, Sherrell RM, Falkowski PG (2001) Iron availability, cellular iron quotas, and nitrogen fixation in *Trichodesmium*. *Limnol Oceanogr* 46(6):1249–1260.
- Kustka AB, et al. (2003) Iron requirements for dinitrogen- and ammonium-supported growth in cultures of *Trichodesmium* (IMS 101): Comparison with nitrogen

- fixation rates and iron:carbon ratios of field populations. *Limnol Oceanogr* 48(5): 1869–1884.
8. Berman-Frank I, Quigg A, Finkel ZV, Irwin AJ, Haramaty L (2007) Nitrogen-fixation strategies and Fe requirements in cyanobacteria. *Limnol Oceanogr* 52(5):2260–2269.
  9. Richier S, et al. (2012) Abundances of iron-binding photosynthetic and nitrogen-fixing proteins of *Trichodesmium* both in culture and *in situ* from the North Atlantic. *PLoS ONE* 7(5):e35571.
  10. Saito MA, et al. (2011) Iron conservation by reduction of metalloenzyme inventories in the marine diazotroph *Crocospaera watsonii*. *Proc Natl Acad Sci USA* 108(6): 2184–2189.
  11. Paerl HW, Prufert-Bebout LE, Guo C (1994) Iron-stimulated N<sub>2</sub> fixation and growth in natural and cultured populations of the planktonic marine cyanobacteria *Trichodesmium* spp. *Appl Environ Microbiol* 60(3):1044–1047.
  12. Moore CM, et al. (2009) Large-scale distribution of Atlantic nitrogen fixation controlled by iron availability. *Nat Geosci* 2(12):867–871.
  13. Wu J, Sunda W, Boyle EA, Karl DM (2000) Phosphate depletion in the western North Atlantic Ocean. *Science* 289(5480):759–762.
  14. Chappell PD, Moffett JW, Hynes AM, Webb EA (2012) Molecular evidence of iron limitation and availability in the global diazotroph *Trichodesmium*. *ISME J* 6(9): 1728–1739.
  15. Sohm JA, Webb EA, Capone DG (2011) Emerging patterns of marine nitrogen fixation. *Nat Rev Microbiol* 9(7):499–508.
  16. Shiozaki T, Furuya K, Kodama T, Takeda S (2009) Contribution of N<sub>2</sub> fixation to new production in the western North Pacific Ocean along 155°E. *Mar Ecol Prog Ser* 377:19–32.
  17. Mills MM, Ridame C, Davey M, La Roche J, Geider RJ (2004) Iron and phosphorus co-limit nitrogen fixation in the eastern tropical North Atlantic. *Nature* 429(6989): 292–294.
  18. Boyd PW, et al. (2007) Mesoscale iron enrichment experiments 1993–2005: Synthesis and future directions. *Science* 315(5812):612–617.
  19. Shi T, Sun Y, Falkowski PG (2007) Effects of iron limitation on the expression of metabolic genes in the marine cyanobacterium *Trichodesmium erythraeum* IMS101. *Environ Microbiol* 9(12):2945–2956.
  20. Falkowski PG (2000) Rationalizing elemental ratios in unicellular algae. *J Phycol* 36(1):3–6.
  21. Millero FJ (1998) Solubility of Fe(III) in seawater. *Earth Planet Sci Lett* 154:323–329.
  22. Jickells TD, et al. (2005) Global iron connections between desert dust, ocean biogeochemistry, and climate. *Science* 308(5718):67–71.
  23. Gao Y, Kaufman YJ, Tanré D, Kolber D, Falkowski PG (2001) Seasonal distributions of aeolian iron fluxes to the global ocean. *Geophys Res Lett* 28(1):29–32.
  24. Vink S, Measures CI (2001) The role of dust deposition in determining surface water distributions of Al and Fe in the South West Atlantic. *Deep Sea Res Part II Top Stud Oceanogr* 48:2787–2809.
  25. Bowie AR, Whitworth DJ, Achterberg EP, Mantoura RF, Worsfold PJ (2002) Biogeochemistry of Fe and other trace elements (Al, Co, Ni) in the upper Atlantic Ocean. *Deep Sea Res Part I Oceanogr Res Pap* 49:605–636.
  26. Measures CI, Landing WM, Brown MT, Buck CS (2008) High-resolution Al and Fe data from the Atlantic Ocean CLIVAR-CO2 Repeat Hydrography A16N transect: Extensive linkages between atmospheric dust and upper ocean geochemistry. *Global Biogeochem Cycles* 22:1–10.
  27. Bergquist BA, Boyle EA (2006) Dissolved iron in the tropical and subtropical Atlantic Ocean. *Global Biogeochem Cycles* 20:1–14.
  28. Noble AE, et al. (2012) Basin-scale inputs of cobalt, iron, and manganese from the Benguela-Angola front to the South Atlantic Ocean. *Limnol Oceanogr* 57(4):989–1010.
  29. Tyrrell T, et al. (2003) Large-scale latitudinal distribution of *Trichodesmium* spp. in the Atlantic Ocean. *J Plankton Res* 25(4):405–416.
  30. Capone DG, Zehr JP, Paerl HW, Bergman B, Carpenter EJ (1997) *Trichodesmium*, a globally significant marine cyanobacterium. *Science* 276(5316):1221–1229.
  31. Großkopf T, et al. (2012) Doubling of marine dinitrogen-fixation rates based on direct measurements. *Nature* 488(7411):361–364.
  32. Subramaniam A, Mahaffey C, Johns W, Mahowald N (2013) Equatorial upwelling enhances nitrogen fixation in the Atlantic Ocean. *Geophys Res Lett* 40(9):1766–1771.
  33. Sañudo-Wilhelmy SA, et al. (2001) Phosphorus limitation of nitrogen fixation by *Trichodesmium* in the central Atlantic Ocean. *Nature* 411(6833):66–69.
  34. Eugster O, Gruber N (2012) A probabilistic estimate of global marine N-fixation and denitrification. *Global Biogeochem Cycles* 26(4):1–15.
  35. Weber T, Deutsch C (2012) Oceanic nitrogen reservoir regulated by plankton diversity and ocean circulation. *Nature* 489(7416):419–422.
  36. Eugster O, Gruber N, Deutsch C, Jaccard SL, Payne MR (2013) The dynamics of the marine nitrogen cycle across the last deglaciation. *Paleoceanography* 28(1):116–129.
  37. Ren H, et al. (2009) Foraminiferal isotope evidence of reduced nitrogen fixation in the ice age Atlantic Ocean. *Science* 323(5911):244–248.
  38. Straub M, et al. (2013) Changes in North Atlantic nitrogen fixation controlled by ocean circulation. *Nature* 501(7466):200–203.
  39. Baker AR, Lesworth T, Adams C, Jickells TD, Ganzeveld L (2010) Estimation of atmospheric nutrient inputs to the Atlantic Ocean from 50°N to 50°S based on large-scale field sampling: Fixed nitrogen and dry deposition of phosphorus. *Global Biogeochem Cycles* 24(3):1–16.
  40. Philander SGH, et al. (1995) Why the ITCZ is mostly north of the Equator. *J Clim* 9: 2958–2972.
  41. Xie S-P, Saito K (2001) Formation and variability of a northerly ITCZ in a hybrid coupled AGCM: Continental forcing and oceanic-atmospheric feedback. *J Clim* 14(6): 1262–1276.
  42. Robinson C, Holligan P, Jickells T, Lavender S (2009) The Atlantic Meridional Transect Programme (1995–2012). *Deep Sea Res Part II Top Stud Oceanogr* 56(15):895–898.
  43. Huffman GJ, et al. (1997) The global precipitation climatology project (GPCP) combined precipitation dataset. *Bull Am Meteorol Soc* 78(1):5–20.
  44. Jickells T (1995) Atmospheric inputs of metals and nutrients to the oceans: Their magnitude and effects. *Mar Chem* 48(3–4):199–214.
  45. Foltz GR, Grodsky SA, Carton JA (2004) Seasonal salt budget of the northwestern tropical Atlantic Ocean along 38°W. *J Geophys Res* 109:1–13.
  46. Da-Allada CY, et al. (2013) Seasonal mixed-layer salinity balance in the tropical Atlantic Ocean: Mean state and seasonal cycle. *J Geophys. Res* 118(1):332–345.
  47. Helmers E, Schrems O (1995) Wet deposition of metals to the tropical North and the South Atlantic Ocean. *Atmos Environ* 29(18):2475–2484.
  48. Measures CI, Vink S (1999) Seasonal variations in the distribution of Fe and Al in the surface waters of the Arabian Sea. *Deep Sea Res Part II Top Stud Oceanogr* 46(8–9): 1597–1622.
  49. Kieber RJ, Hardison DR, Whitehead RF, Willey JD (2003) Photochemical production of Fe(II) in rainwater. *Environ Sci Technol* 37(20):4610–4616.
  50. Shi Z, et al. (2012) Impacts on iron solubility in the mineral dust by processes in the source region and the atmosphere: A review. *Aeol Res* 5:21–42.
  51. Kieber RJ, Skrabal SA, Smith BJ, Willey JD (2005) Organic complexation of Fe(II) and its impact on the redox cycling of iron in rain. *Environ Sci Technol* 39(6):1576–1583.
  52. Fernandez A, Morino-Carballido B, Bode A, Varela M, Maranon E (2010) Latitudinal distribution of *Trichodesmium* spp. and N<sub>2</sub> fixation in the Atlantic Ocean. *Biogeochemistry* 7(10):3167–3176.
  53. Tyrrell T (1999) The relative influences of nitrogen and phosphorus on oceanic primary production. *Nature* 400:525–531.
  54. Dutkiewicz S, Ward BA, Monteiro F, Follows MJ (2012) Interconnection of nitrogen fixers and iron in the Pacific Ocean: Theory and numerical simulations. *Global Biogeochem Cycles* 26(1):1–16.
  55. Ward BA, Dutkiewicz S, Moore CM, Follows MJ (2013) Iron, phosphorus and nitrogen supply ratios define the biogeography of nitrogen fixation. *Limnol Oceanogr* 58(6): 2059–2075.
  56. Palter JB, Lozier MS, Sarmiento JL, Williams RG (2011) The supply of excess phosphate across the Gulf Stream and the maintenance of subtropical nitrogen fixation. *Global Biogeochem Cycles* 25(4):1–14.
  57. Knapp AN, DiFiore PJ, Deutch C, Sigman DM, Lipschultz F (2008) Nitrate isotopic composition between Bermuda and Puerto Rico: Implications for N<sub>2</sub> fixation in the Atlantic Ocean. *Global Biogeochem Cycles* 22(3):1–14.
  58. Moore JK, Doney SC (2007) Iron availability limits the ocean nitrogen inventory stabilizing feedbacks between marine denitrification and nitrogen fixation. *Global Biogeochem Cycles* 21:1–12.
  59. Monteiro FM, Dutkiewicz S, Follows MJ (2011) Biogeographical controls on the marine nitrogen fixers. *Global Biogeochem Cycles* 25(2):1–8.
  60. Giovannoni SJ, Vergin KL (2012) Seasonality in ocean microbial communities. *Science* 335(6069):671–676.
  61. Longhurst AR (2007) *Ecological Geography of the Sea* (Academic Press, San Diego), 2nd Ed.
  62. Lenes JM, et al. (2001) Iron fertilization and the *Trichodesmium* response on the West Florida shelf. *Limnol Oceanogr* 46(6):1261–1277.
  63. Benavides M, Aristegui J, Agawin NSR, Cancio JL, Hernandez-Leon S (2013) Enhancement of nitrogen fixation rates by unicellular diazotrophs vs. *Trichodesmium* after a dust deposition event in the Canary Islands. *Limnol Oceanogr* 58(1):267–275.
  64. Schmidt MW, Spero HJ (2011) Meridional shifts in the marine ITCZ and the tropical hydrologic cycle over the last three glacial cycles. *Paleoceanography* 26(1):PA1206.
  65. Meckler AN, et al. (2011) Deglacial nitrogen isotope changes in the Gulf of Mexico: Evidence from bulk sedimentary and foraminifera-bound nitrogen in Orca Basin sediments. *Paleoceanography* 26(4):1–13.
  66. Redfield AC, Ketchum BH, Richards FA (1963) The influence of organisms on the composition of sea water. *The Sea*, ed Hill MN (Wiley-Interscience, New York), Vol 2, pp 26–77.
  67. Landolfi A, Dietze H, Koeve W, Oshlies A (2013) Overlooked runaway feedback in the marine nitrogen cycle: The vicious cycle. *Biogeochemistry* 10:1351–1363.
  68. Canfield DE (2006) Models of oxic respiration, denitrification and sulfate reduction in zones of coastal upwelling. *Geochim Cosmochim Acta* 70(23):5753–5765.
  69. Zhang J-Z, Chi J (2002) Automated analysis of nanomolar concentrations of phosphate in natural waters with liquid waveguide. *Environ Sci Technol* 36(5):1048–1053.
  70. Obata H, Karatani H, Nakayama E (1993) Automated determination of iron in seawater by chelating resin concentration and chemiluminescence detection. *Anal Chem* 65:1524–1528.
  71. Brown MT, Bruland KW (2008) An improved flow-injection analysis method for the determination of dissolved aluminum in seawater. *Limnol Oceanogr Methods* 6: 87–95.
  72. Montoya JP, Voss M, Kahler P, Capone DG (1996) A simple, high-precision, high-sensitivity tracer assay for N<sub>2</sub> fixation. *Appl Environ Microbiol* 62(3):986–993.
  73. Voss M, Croot P, Lochte K, Mills M, Peeken I (2004) Patterns of nitrogen fixation along 10°N in the tropical Atlantic. *Geophys Res Lett* 31(23):L23S09.